

Estimating in situ phytoplankton growth rates with a Lagrangian sampling strategy

Ingrid Hillmer^{1,2} and Jörg Imberger¹

¹Centre for Water Research, The University of Western Australia, 35 Stirling Highway, Crawley 6009, Western Australia, Australia

²Department of Civil Engineering, University of Chile, Av. Blanco Encalada 2002, Casilla 228 – 3, Santiago, Chile

Abstract

Quantification of biogeochemical rates is essential to the understanding of the dynamics of aquatic ecosystems. However, this has proven to be difficult to achieve especially under conditions of high spatial and temporal hydrodynamic and biogeochemical variability. Here, a Lagrangian experimental design was employed to estimate biogeochemical rate coefficients in situ. A set of four drogues and a cross-transect sampling design was used to capture the patchy distribution of phytoplankton and nutrient species, and high transport and mixing rates. A mass balance approach was applied to a Lagrangian control volume moving with a drogue. This approach was used to separate internal biogeochemical changes from the physical changes due to advection, diffusion, and convergence/divergence fluxes. This experimental approach was applied to an oligotrophic coastal region. The phytoplankton growth rate, primary production, and carbon to chlorophyll ratio (C:Chla) obtained from the experiment agreed with the highest literature values for this study site. This supported the validity of this approach. The effect of scales of processes and patchiness is highlighted from this experiment. It is shown that the experimental design is subject to a relationship between size of the control volume, the time scale of internal processes, and sampling time.

Determining the fluxes of mass and energy through the different components of the ecological cycle is a central issue in aquatic ecological research. Different approaches have been used in different ecosystems; however, the success in the quantification of the internal biogeochemical processes of nutrient cycles and phytoplankton dynamics could be considered limited in some study cases.

A common approach used for estimating internal biological and chemical flux paths has been to enclose the natural biological populations in bottles suspended in situ. After an incubation period (~hours/days), changes in biological and nutrient concentrations allow the determination of the rate of processes such as nutrient uptake, phytoplankton growth, and primary production. However, extrapolation of these results to

the ambient environment is questionable because, for instance, physical processes (e.g., turbulence and vertical movements) are totally altered in such enclosures. For example, bottle experiments can mask significant variability in the photosynthetic rates of individual phytoplankton cells because of constant versus variable light climate in natural conditions (Marra 1978*a*, 1978*b*, 1980). Further, the limited number of samples may not be representative of the spatial heterogeneity in the ambient environment.

Many investigators have obtained estimates of ecosystem budgets for different biological species with a mass balance method (e.g., Odum 1956; Smith and Atkinson 1983, 1984; D'Avanzo et al. 1995). This technique, however, suffers from difficulties and restrictions. For instance, the large uncertainties in estimating the movement of mass carried by the water flow through open system boundaries can lead to significant errors in systems where advective fluxes are important. In addition, budgets sometimes are calculated over seasonal or annual scales. And thus, varying details of internal fluxes within the system remain unclear as the sampling strategy does not capture the spatial and temporal scales associated with the internal processes (Platt and Denman 1975; Imberger et al. 1983; Smith 1984; Kraines et al. 1996).

The mass balance technique has been applied to calculate rates of processes in different situations. For instance, net production has been inferred from chemical data in well-defined

Acknowledgments

The development of the field experiment was made possible through the technical and logistical support provided by the Field Operations Group, Centre for Water Research, The University of Western Australia (Sheere Feaver, Carol Lam, Roger Head, and Greg Attwater) and by the partial funding provided by the Water Corporation, Western Australia. We would like to thank Krsysztof Wienczugow (Marine and Freshwater Research Laboratory, Institute for Environment Science, Murdoch University) for kindly providing his expertise during the fieldwork. We also wish to thank Jordan Furnans, Patricia Okley, and Peter Yeates for help provided on many different levels during the 4-d experiment. We also appreciate the helpful reviews by Richard Segal, Tamar Zohary, and Jose Romero.

water masses such as fjords and coral reefs (Broenkow 1965) assuming that horizontal advection and diffusion may be disregarded. In particular areas, such as in upwelling regions, flux estimates have been inferred by calculating the deviation from the behavior of a conservative tracer (Minas et al. 1986). In this case, the assumptions and time scales of sampling allow questions to be addressed only at the system level and not at the level of specific biogeochemical processes. The mass balance also has been applied to specific control volumes or well-defined domains using higher temporal resolution (e.g., hours/days). Odum (1956) determined primary productivity by measuring dissolved oxygen in a segment of a stream. A whole-lake approach has been used in small lakes to study primary productivity and respiration (Melack 1982) and the metabolic balance (Cole et al. 2000), both using dissolved oxygen flux estimates, and to determine the factors regulating the abundance and productivity of bacteria (Pace and Cole 1996). In all these cases, some considerations about the horizontal advection and mixing were taken into account.

As the level of complexity of the systems and of the questions to be addressed increases, it becomes necessary to increase the sophistication of the experiment design and the technology used. Recently, for instance, the *in situ* stable isotope tracer techniques have yielded improved understanding of nitrogen processes under natural conditions in well-defined domains (Tobias et al. 2003; Gribsholt et al. 2005). In the case of complexities generated in open systems, the use of the control volume approach has proved to be an appropriate tool to resolve, together with the right equipment, the fate of substances and the rate of processes. For instance, a phosphorus budget has been calculated in the epilimnetic waters of a small lake to determine the balance between imported and recycled production (Caraco et al. 1992). In addition, Genin et al. (2002) defined a control volume to measure *in situ* biogeochemical fluxes and to determine the phytoplankton grazing at the scale of the coral reefs. In this case, the method used allowed eliminating the interference and limitations imposed by assumptions and artifacts that otherwise would be necessary to apply.

The difficulties imposed by the presence of advection in the calculation of a substance mass balance have been overcome, in some studies, by the application of the Lagrangian approach. This approach removes the signal of the advective process from the measurements by keeping track of the same parcel of water. Over sampling frequencies of days to weeks, this method has been applied to studies with a variety of objectives. For instance, to study the response of phytoplankton to a new source of nitrogen from upwelling (Dortch and Postel 1989), nutrient cycling in a phytoplankton bloom (Ketchum and Corwin 1965), to estimate productivity and gas exchange (Wanninkhof et al. 1997), assess response to a *P* addition in a *P*-deficient environment (Thingstad et al. 2005), and to investigate the generation of algal blooms (Park et al. 2005). However, if a single drogue is used to track the Lagrangian parcel of water, changes in concentration due to

horizontal and vertical mixing cannot be quantified for the mass balance, unless their effect could be disregarded. This should be particularly evident in frontal zones where mixing, downwelling, and upwelling alter the identity of the water masses. Thus, to take into account the horizontal dispersion, some studies have removed its effect by injecting a conservative gas tracer (Wanninkhof et al. 1997; Park et al. 2005; Thingstad et al. 2005). And in the *in situ* iron enrichment experiment (Coale 1998), a combination of both strategies, a buoy and a tracer, were used to track the patch and investigate the biological and chemical changes within it.

The essential issue in any ecological study, either based on field or numerical data, is to understand the hierarchy of biogeochemical and physical processes to ensure that measured fluxes are not overwhelmed by unaccounted fluxes (Imberger et al. 1983; Smith 1984; Hillmer and Imberger, 2007). Hence, the design of ecological experiments must ensure that physical processes are not masking the biogeochemical changes in the biological species and nutrient concentrations. In other words, the spatial and temporal scales of physical processes must be equal to or greater than the scales of biogeochemical processes responsible for biological and chemical variability. Further, consideration must be given to patchiness resulting from the interaction between physical and biogeochemical processes and their transient nature to correctly interpret the data (Dutilleul 1993).

The complexity of physical processes of coastal areas, such as strong advective and dispersive fluxes that interact with patches, increases the difficulty in determining the internal variability. To compensate for this, a new Lagrangian experiment is proposed here. The experiment was applied to a shallow coastal area off Perth in the southern-west coast of Western Australia. This experiment was carried out in the vicinity of a sewage discharge to estimate growth rates in response to the injection of nutrients. In this Lagrangian approach, a control volume is defined that moves with a drogue located at its center. The internal rates are estimated by applying a mass balance to this control volume. The different terms in the conservation-of-mass equation are obtained from vertical measurements carried out at sampling stations in a cross-transect formation, the spreading rate of a set of four drogues, the mass balance of a conservative tracer, salinity, and microstructure measurements. The experiment is designed to remove the effects of both advection and horizontal dispersion, allowing the determination of phytoplankton growth rates at temporal and spatial scales of hours and hundreds of meters, respectively.

Materials and procedures

Lagrangian experimental design—Three drogues (D2, D3, and D4) were launched in an equilateral triangular formation with a fourth drogue, or central drogue (CD), at the center of the triangle (Fig. 1). Each corner of the formation was approximately 150 m from the center. The drogues were designed with two sets of vertical metal frames 2 m high, covered with

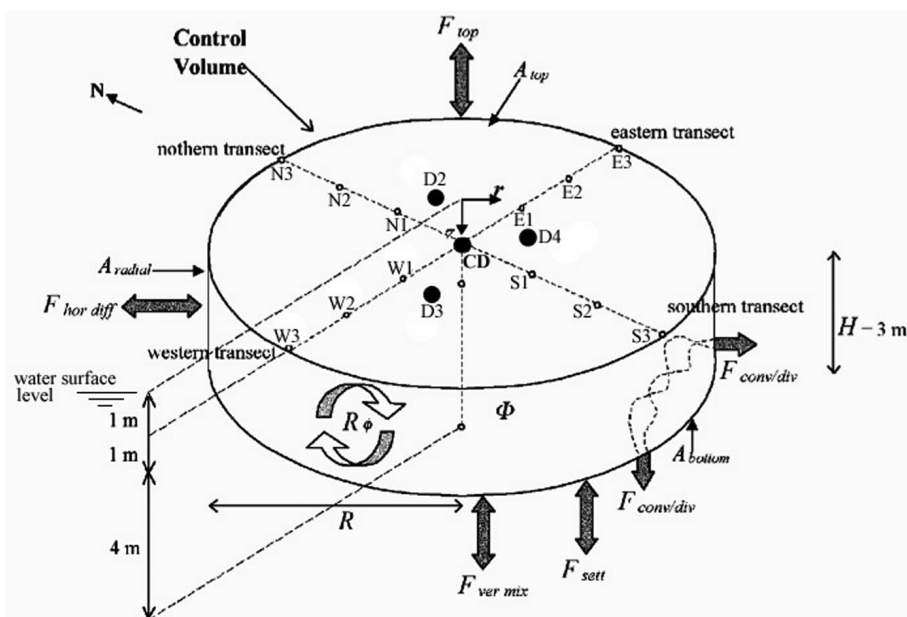


Fig. 1. Scheme of the experiment design, showing the control volume, the drogues' initial arrangement (●; CD, D2, D3, and D4), the sampling stations (○; N_i , S_i , E_i , W_i ; $i = 1, 2, 3$), and the internal and external fluxes. Φ represents the concentration of a biological or chemical species, R_ϕ is the rate of internal biogeochemical changes, $F_{hor\ diff}$ represents the fluxes due to horizontal diffusion across the radial surface A_{radial} of the control volume, and $F_{con/div}$ represents the advective fluxes across the surface A_{bottom} and A_{radial} . $F_{ver\ mix}$ and F_{sett} represent the fluxes due to vertical mixing and due to settling, respectively, across the bottom surface, A_{bottom} , and top surface, A_{top} . In the figure, F_{top} represents the combination of $F_{ver\ mix}$ and F_{sett} across the surface A_{top} . H is the height and R the radius of the control volume.

plastic sheeting as drag elements, and deployed at 2 m depth. Each drogue was equipped with a GPS data logger that registered the position every 10 s.

The sampling strategy was based on repeated transects that formed a cross across the CD (Fig. 1). Each cross-transect consisted of four transects oriented toward the north (N), south (S), east (E), and west (W) from the central drogue with three sampling stations set along each transect (N_i , S_i , E_i , W_i ; $i = 1, 2, 3$ where i indicates the position in the transect moving outwards as i increases; Fig. 1). The interval between each sampling station was approx. 150 m.

Vertical profiles—Vertical profiles of temperature, salinity, dissolved oxygen (DO), and turbidity were obtained using a fine-scale profiler (F-Probe) at the 12 sampling stations in each cross-transect. Vertical profiles of phytoplankton biomass (chlorophyll *a*) were measured using a spectrofluorometer (BBE Fluoroprobe) attached to the probe mentioned previously. The Fluoroprobe results were compared with measurements of extracted chlorophyll *a* (Chl *a*) (see Assessment).

Meteorological data—Meteorological parameters were collected in the study area using the Lake Diagnostic System (LDS, developed at the Centre for Water Research) that was located approximately 500 m offshore from the end of the outfall (Fig. 2). The station included wind speed and direction sensors, net solar radiation, short wave radiation, relative humidity, and air temperature sensors. Only wind data are used in this study. Wind data from the Ocean Reef meteorological station situated inshore also was used (see below; Fig. 2).

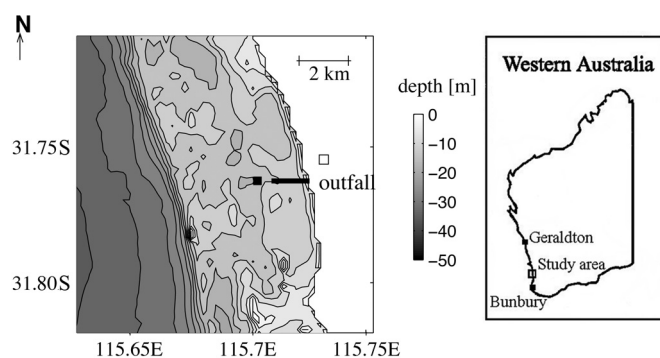


Fig. 2. Location and bathymetry of Whitford's Lagoon showing the approximate position of the outfall (—), the Ocean Reef meteorological station (□), and the LDS station (■).

Mass balance in a fixed control volume—A Lagrangian control volume (CV) was defined as a cylinder with the CD at its center (Fig. 1). The control volume was limited to 3 m depth, minimizing the effects of any non-uniformity due to a vertical variation in the horizontal velocity. The top of the CV was situated at 1 m below the water surface ($z = 1$ m); the rough surface conditions due to the presence of waves increased the difficulties during the measurements causing the absence of data for the first top meter in most of the profiles. The bottom of the CV was at $z = 4$ m. The radius R , was defined as the minimum distance between the center (CD) and the furthest sampling point in each transect (N_3 , S_3 , E_3 , and W_3) recorded that day.

A mass balance was applied to the Lagrangian control volume to obtain a residual term to keep the balance between the measured fluxes and the rate of change of the species of interest, Φ . Each term was evaluated for the m^{th} cross-transect as follows:

$$\frac{\Delta\Phi^m}{\Delta t} \Big|_{CV} = \Delta\Phi_{hor\ diff}^m + \Delta\Phi_{ver\ mix}^m + \Delta\Phi_{conv/div}^m + \Delta\Phi_{res}^m \quad (1)$$

where $\Delta\Phi_{res}^m = \Delta\Phi_{bio}^m + \Delta\Phi_{sett}^m$ is the residual term. $\Delta\Phi_{bio}^m$ represents the volume-averaged internal biogeochemical reaction rate and is zero for conservative tracers. The flux due to settling, through the top and bottom of the control volume, $\Delta\Phi_{sett}^m$ is relevant only for particulate matter such as phytoplankton. $\Delta\Phi_{hor\ diff}^m$ is the horizontal diffusion flux across the radial boundary and $\Delta\Phi_{ver\ mix}^m$ is the flux due to vertical mixing across the top and bottom surfaces. It was assumed that the cylindrically shaped control volume moved as a solid body with the velocity of the central drogue, so that any divergent or convergent flow relative to the central drogue would lead to an advective flux, $\Delta\Phi_{conv/div}^m$, across the vertical and side boundaries.

The mean concentration inside the CV, Φ^m , was calculated by averaging the vertically integrated concentration from the 12 sampling stations ($N_i, S_i, E_i, W_i; i = 1, 2, 3$; Fig. 1) obtained for the m^{th} cross-transect. $\Delta\Phi^m$ was obtained from the difference between Φ^{m+1} and Φ^m , and the temporal interval between two cross-transects was given by $\Delta t = t^{m+1} - t^m$. t^m was calculated as the average between the time for the first measurement and the last measurement in the m^{th} cross-transect.

The net horizontal diffusive flux per unit volume ($\Delta\Phi_{hor\ diff}^m$) was calculated as the average between the northern, southern, western, and eastern flux as following:

$$\Delta\Phi_{hor\ diff}^m = k_h \frac{S_i}{V} \sum_{i=1}^4 \frac{\Delta\Phi_i}{\Delta R_i} = k_h \frac{1}{2R} \sum_{i=1}^4 \frac{\Phi_{i3} - \Phi_{i2}}{R_{i3} - R_{i2}} \quad (2)$$

where k_h is the horizontal diffusion coefficient and i indicates the four cardinal points (N, S, W, and E; Fig. 1). R_{ij} is the distance from the CD to the sampling point j in the transect i . A_i was the area associated with the flux in the i direction and is equal to $2\pi RH/4$. k_h was obtained from the drogue data analysis and from the salinity equation as explained below.

The vertical gradient was estimated from the vertical profiles at the 12 sampling stations in each cross transect ($N_i, S_i, E_i, W_i; i = 1, 2, 3$; Fig. 1) at $z = 1$ and 4 m. The first derivative of the variable Φ in the vertical profile was calculated with a Gaussian derivative 31-point filter. The microstructure data were used to determine an estimate of the vertical diffusion coefficient from the dissipation measurements as described below. The gradient of the variable of interest, Φ , obtained at the bottom and top of the control volume in each sampling point, was averaged and then multiplied by the corresponding area and the vertical diffusion coefficient, assuming a homogeneous coefficient, to get the vertical flux for that cross-transect.

The advective flux is equal to $\Delta\Phi_{conv/div}^m = (\Phi_o - \Phi)Q$ where Φ_o is the concentration outside the CV and Q is the net volume flux of water coming into and going out of the CV due to the

divergence/convergence of the flow. This flux was calculated using the conservation of mass for salinity, in which case $\Delta\Phi_{res}^m = 0$. Using the diffusion coefficient obtained from the drogues' analysis to calculate the diffusive fluxes (Eq. 2), the only unknown term in Eq. 1 is then $\Delta\Phi_{conv/div}^m$.

Horizontal diffusion coefficient—The rate of spreading of the drogues was used to estimate the horizontal dispersion coefficient. The standard deviation of the distribution of the drogues in the x (west–east) and y (south–north) direction (σ_x and σ_y) are used to calculate the two-dimensional standard deviation $\sigma_{xy} = (\sigma_x^2 + \sigma_y^2)^{1/2}$ and the dispersion coefficient as $k_i = 0.5 d\sigma_i^2/dt$, with t the time and $i = x, y$, and xy (Fischer et al. 1979; Stocker and Imberger 2003).

The mass balance equation (Eq. 1) for salinity also was used to estimate a horizontal diffusion coefficient. In this case, however, it was assumed that the divergent/convergent fluxes were small and can be disregarded ($\Delta\Phi_{conv/div}^m = 0$) and thus the only unknown term was $\Delta\Phi_{hor\ diff}^m$. Equation 2 then is used to calculate the diffusion coefficient. Diffusion coefficients obtained from the conservation of salinity and the assumptions made, were compared with the ones obtained from the drogues' analysis to validate them and understand the dynamic of the control volume (see Assessment).

Microstructure data—A microstructure profiler equipped with a pressure sensor, a fast-response temperature-conductivity sensor, and an accurate temperature-conductivity sensor was used to document the dissipation of turbulent kinetic energy (Luketina and Imberger 2001) at the central drogue position. The probe was deployed in falling mode, with the probe descending freely with a constant velocity of around 0.1 ms^{-1} . The sampling rate used, 100 Hz, yielded a vertical spatial resolution of the sensors of 1 mm.

The vertical turbulent diffusivity (k_z) was calculated as $k_z = R_f (1 - R_f)^{-1} \epsilon N^{-2}$ (Osborn 1980), where ϵ is the rate of energy dissipation, R_f is the flux Richardson number or mixing efficiency, and $N = (-g/\rho\partial\rho/\partial z)^{-0.5}$ is the buoyancy frequency, with g and ρ the gravity and density respectively. The rate of energy dissipation was computed by a least-squares fit of the power spectral salinity-gradient signal to the Batchelor spectrum (Imberger and Ivey, 1991; Luketina and Imberger 2001) from the microstructure data. In this study, R_f was assumed to have a value of 0.2 (thus $k_z = 0.25\epsilon N^{-2}$). This value corresponds to the upper limit for the R_f variation (Ivey and Imberger 1991), meaning that there is a maximum efficiency of conversion of the net mechanical energy required to sustain turbulent motions to the buoyancy flux. Given that the turbulence was energized by the surface wind and therefore expected to be active, this assumption is quite reasonable.

Assessment

Experimental setup—A 4-d field experiment was carried out in Whitfords Lagoon located in Marmion Marine Park on 21 March (day 1) and 25, 26, and 27 March 2003 (day 2, 3, and 4, respectively). The objective of the experiment was to estimate

in situ rates for phytoplankton growth by isolating them from the transport and mixing effects. The study area is a shallow semi-enclosed lagoon off Perth, located on the south-west coast of Western Australia (31.75°S, 115.75°E; Fig. 2). The presence of submerged limestone reefs creates an irregular topography with a mean depth of 10 m and with a partial open ocean boundary. The wind is the main mechanism driving the currents in the area.

The study area is an oligotrophic system with N:P ranging from <1:1 in summer to approx. 3:1 in winter (Lord 2000); unusually low by world standards. The area receives freshwater and nutrient input from groundwater (Johannes 1985) and from a wastewater treatment plant through an outfall, 1820 m long, with a 200 m long diffuser at approximately 10 m depth (Fig. 2). The mean effluent discharge is 0.7 m³s⁻¹, with a minimum discharge of 0.25 m³s⁻¹ in the morning and a peak of 1.1 m³s⁻¹ in the afternoon. The associated nutrient concentrations of the effluent are approximately 2.1 mmoles N L⁻¹, 0.1 mmoles N L⁻¹, and 1.6 mmoles N L⁻¹ for total nitrogen (TN), ammonium (NH₄) and nitrate + nitrite (NO_x), respectively. The N:P ratio of the treated wastewater is about 5:1 which maintains the strong nitrogen limitation found in phytoplankton in the area (Lord 2000). Throughout the year, the composition of the phytoplankton species is dominated by diatoms (Lord 2000).

The four drogues (CD, D2, D3, and D4) were launched in the vicinity of the outfall in the morning and retrieved at the

Table 1. Schedule of cross-transect sampling and microstructure profiling.

Day#	Day	Cross-transect (CT)	t _i (h) – t _f (h)* CT	t _i (h) – t _f (h)* Microstructure
1	21 March	1	0701 – 0817	0858 – 0919
		2	0929 – 1051	1112 – 1125
		3	1204 – 1312	1321 – 1337
2	25 March	1	0644 – 0743	0752 – 0805
		2	0816 – 0919	0930 – 0951
		3	1013 – 1110	1117 – 1129
		4	1215 – 1321	1328 – 1340
		5	1352 – 1507	1528 – 1540
3	26 March	1	0635 – 0819	
		2	0819 – 0956	
		3	0956 – 1209	
		4	1209 – 1352	
		5	1352 – 1543	
4	27 March	1	0638 – 0758	
		2	0758 – 0942	
		3	0942 – 1117	
		4	1117 – 1257	
		5	1257 – 1420	
		6	1420 – 1554	
		7	1554 – 1700	

*t_i and t_f denote the initial and final time for the probes measurements and collection of water samples in each transect.

end of each day, mainly to avoid losing them. The freshwater outfall discharge caused a salinity gradient that provided a natural tracer. The high nutrient loads from the outfall stimulated the phytoplankton growth that enhanced signal-to-noise ratio in the algal level. The experiment was conducted over 6 to 10 hours a day (from 600 to 1600 h approx.; Table 1). On day 1, the GPS data from the data loggers was irretrievable, and data which was transmitted by phone every 30 min was used. On day 3, problems with the data logger of one of the drogues occurred, so its position was recorded with the GPS on the boat. The meteorological station was installed on 20 March 2003 (Fig. 2).

The start of each transect was based on the position of the CD. The coordinates from the CD were recorded at the beginning of each transect and used to set the three sampling points in a straight line toward each of the cardinal points (N1–N3, S1–S3, E1–E3, W1–W3; Fig. 1). After finishing a transect, the new position of the CD was recorded and the sampling points in the next transect were set following the same procedure. For the subsequent analysis, the relative position of each sampling point was calculated with respect to the actual position of the CD at the time of the measurement. The sampling frequency for the cross-transects varied between 1.5 to 2.5 h. Five microstructure deployments were carried out at the CD location at the end of each cross-transect during day 1 and day 2 (Table 1).

Biological and chemical data—Samples for phytoplankton identification and enumeration, and Chl *a* analysis were collected for verification of Chl *a* fluorescence profiles from the probe deployed at the same time. Phytoplankton samples were collected at 2 and 6 m depth at the location of the CD position on day 3 and day 4. Samples were collected in the second and fifth cross-transect on day 3, and in the second and fourth cross-transect on day 4. Samples were collected through pumping water at a specific depth into plastic buckets on the boat. The samples for Chl *a* analysis were filtered immediately afterward through glass fiber filter (nominal pore size 0.9 – 1.2 μm). Filters were stored on ice and in the dark, and frozen upon return to the laboratory. Chl *a* was determined by grinding thawed filters in 90% acetone, followed by trichromatic spectrophotometric determination (Strickland and Parsons 1972, Greenberg et al. 1992). The samples for phytoplankton identification and enumeration analysis were preserved and stored on ice and in a dark place and then stored in the dark and under refrigeration upon return to the laboratory. The subsequent analysis was carried out using the Utermöhl method (Utermöhl 1958) and an inverted microscope at 500× magnification.

Water samples also were collected for subsequent analysis of nitrate + nitrite (NO_x-N), ammonium (NH₄-N), total dissolved nitrogen (TDN), and total nitrogen (TN). These data were used for further assessment of the approach proposed in this study. Six samples for the nitrogen analysis were collected in each cross-transect by means of pumping water as for the Chl *a* samples. The samples were collected at 2 m and 6 m at

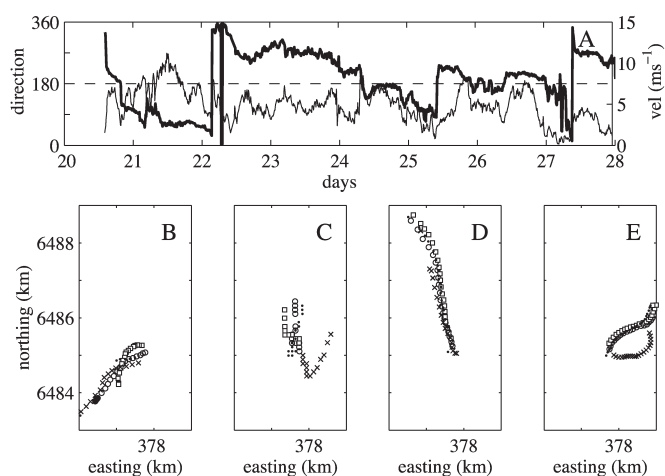


Fig. 3. LDS wind data and drogues' trajectories during the 4-d experiment. A) Wind direction (clockwise from north; thick line) and magnitude (thin line) from 20 to 28 March 2003. Wind data from the Ocean Reef meteorological station situated inshore was used between 21.09 and 22.45 due to failures in the equipment. B) 21 March 2003 (day 1), C) 25 March 2003 (day 2), D) 26 March 2003 (day 3), and E) 27 March 2003 (day 4). The symbol \circ represents the position of CD, \square represents the position of D2, \bullet represents the position of D3, and \times represents the position of D4.

the location of CD, and at 2 m at N3, S3, W3, and E3 (Fig. 1). Samples for NO_x , NH_4 , and TDN analysis were syringe filtered through $0.45 \mu\text{m}$ membrane filters into polypropylene tubes and, together with the water samples for TN analysis, were stored on ice and in the dark. All samples were frozen upon return to the laboratory. NO_x was analyzed by the copper-cadmium reduction method (Johnson 1983), NH_4 by the alkaline phenate method (Switala 1993), and TN and TDN by autoclave digests with potassium persulphate (Valderrama 1981). All analyses were carried out using a Lachat Automated Flow Injection Analyser. Due to problems with the pump on day 1, only water from the surface was collected in the second and third cross-transect for nitrogen and chlorophyll *a* analysis.

Consequences of the relative movement of the drogues—The movement of the drogues varied according to the wind field (Fig. 3). There was a high correlation between wind stress and the current field when the alongshore component was strong (Fig. 3B, D; Zaker 1998). Under this condition, the four drogues were transported in the same direction as a relatively high cohesive group. The dominance of the wind declined when the alongshore wind stress was weak or the cross-shore wind component was large. In these cases, topographical constraints affected the motion in the lagoon generating local currents (Fig. 3C, E; Zaker 1998). In these situations, the formation of the drogues tended to lose its cohesive integrity or identity when one of the drogues moved apart from the main group. In turn, this may lead to a loss of identity of the control volume caused by high advective fluxes. These fluxes may replace, partly or totally, the mass of water (*see* next section) in the control volume.

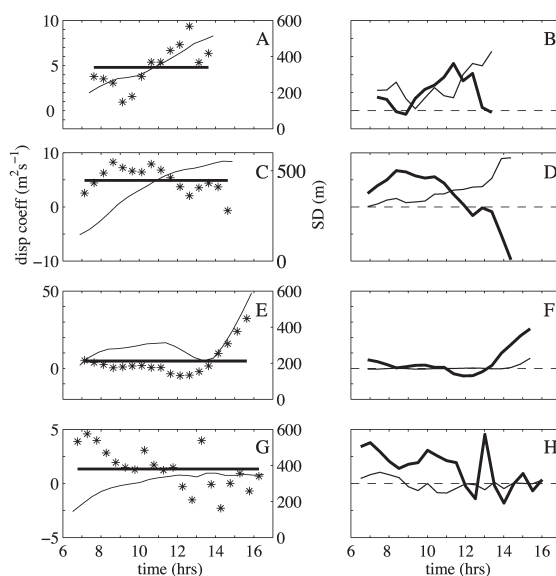


Fig. 4. Temporal evolution of the horizontal dispersion coefficient and standard deviation of the distribution of the drogues for each day. Horizontal dispersion coefficient, mean value, and standard deviation: A) 21 March 2003 (day 1), C) 25 March 2003 (day 2), E) 26 March 2003 (day 3), and G) 27 March 2003 (day 4). The symbol $*$ represents the horizontal dispersion coefficient obtained from the divergence of the drogues, the thick line represents the daily averaged horizontal dispersion coefficient, and the thin line represents the standard deviation of the distribution of the drogues. Horizontal dispersion coefficient in the x (west–east, thin line) and y (south–north, thick line): B) 21 March 2003 (day 1), D) 25 March 2003 (day 2), G) 26 March 2003 (day 3), and H) 27 March 2003 (day 4). Thin line represents dispersion coefficient in the x direction and thick line dispersion coefficient in the y direction.

The variance of the distribution of the drogues increased most of the time (Fig. 4) with a variable rate of dispersion. The values for the dispersion coefficient obtained from the drogues are in agreement with values found previously in the area (Pattiaratchi and Knock 1995; Zaker 1998) with a mean value for each day of 4.8 , 4.9 , 4.8 , and $1.3 \text{ m}^2\text{s}^{-1}$ (d 1, d 2, d 3, and d 4, respectively; Fig. 4) and a 4-d mean for the experiment of $4.0 \text{ m}^2\text{s}^{-1}$.

The rate of spreading of the drogues has been separated into the directions x and y (WE and SN respectively; Fig. 4) to analyze the divergent/convergent fluxes (div/conv) across the control volume boundaries. The div/conv fluxes occurred in two different ways: the rate of spreading in x and y direction added their effect (i.e., they had the same sign) or they had opposite effect (different signs). In the first case, the volume of water underwent a lateral expansion or contraction that produced a vertical and lateral flux of water passing through the rigid CV. In the second situation, lateral fluxes caused by the lateral stretching combined with the vertical and lateral fluxes due to the expansion and contraction (only lateral fluxes can be expected if the flow undergoes purely lateral stretching deformation). In some cases, the variance and dispersion coefficients increased, but the formation of the drogues had lost its integrity.

Table 2. Terms of the conservation of salinity (S) equation calculated between cross-transects (CT) measured at time t in a control volume defined by the radius R and height H .

Day	CT	R (km)	H (m)	t hours	S (psu)	$\Delta S/\Delta t$ (psu)s ⁻¹ (1)	$\Delta S_{hor\ diff}(k_h)^{-1}$ (psu)m ⁻² (2)	k_v m ² s ⁻¹ (3)	$\Delta S_{ver\ mix}(k_v)^{-1}$ (psu)m ⁻² (4)
1	1	0.217	3.0	7.7	36.013	8.0E-06	4.5E-06	7.3E-05	1.6E-02
	2			10.2	36.086	3.5E-06	6.9E-07	2.2E-03	6.8E-04
	3			12.6	36.117				
2	1	0.254	3.0	7.2	36.046	-2.7E-06	2.3E-07	1.2E-03	-3.6E-04
	2			8.8	36.031	1.5E-06	-1.7E-06	1.2E-03	1.0E-02
	3			10.7	36.041	1.8E-07	-8.1E-07	6.8E-04	5.5E-03
	4			12.8	36.043	2.6E-06	-5.8E-07	6.8E-04	4.7E-03
	5			14.5	36.059				
3	1	0.221	3.0	7.4	35.994	1.9E-06	-5.5E-07	1.3E-03	1.2E-02
	2			9.3	36.008	-2.8E-07	8.6E-07	1.3E-03	2.1E-03
	3			11.0	36.006	1.4E-06	1.8E-07	1.3E-03	9.6E-03
	4			12.9	36.016	-1.0E-04	1.8E-07	1.3E-03	-1.3E-03
	5			15.0	35.218				
4	1	0.226	3.0	7.3	35.054	8.7E-05	2.0E-07	6.8E-04	1.3E-02
	2			8.9	35.576	7.8E-05	1.2E-05	6.8E-04	1.0E-02
	3			10.5	36.009	-8.6E-08	-8.8E-07	6.8E-04	9.0E-03
	4			12.1	36.009	-4.3E-06	2.5E-07	6.8E-04	3.0E-03
	5			13.6	35.985	-3.9E-06	-6.6E-07	6.8E-04	-7.9E-03
	6			15.1	35.965	-1.0E-06	-2.1E-07	6.8E-04	2.3E-02
	7			16.5	35.960				

*psu, practical salinity units; $\Delta S/\Delta t$, temporal change in concentration in the control volume; $\Delta S_{hor\ diff}$, changes due to horizontal diffusion; k_h , horizontal diffusion coefficient; k_v , vertical diffusion coefficient; $\Delta S_{ver\ mix}$, changes due to vertical mixing.

The dynamic of the CV for each cross-transect was classified based on the characteristics of the relative movement of the drogues (Fig. 3 and Fig. 4), into a divergence case (a positive spread in both directions), convergence case (a negative spread in both directions), divergence/convergence (opposite sign in both directions), and loss of integrity. Divergent flows characterized the dynamic on day 1, with similar rate of spreading in both directions. On day 2, a divergent dynamic dominated although a loss of integrity of the drogues was detected during the first cross-transect. Day 3 and day 4 presented a combination of divergent and convergent flows without a clear dominance of any of them. In both days also a loss of identity of the drogues' formation occurred.

Removal of the interference of the div/conv fluxes using salinity mass balance—As explained above, the mass balance of the salinity tracer (Eq. 1; $\Delta S_{res} = 0$), with the horizontal diffusion coefficient obtained from the spread of the drogues, was used to estimate $\Delta S_{conv/div}$ and subsequently the divergent and convergent flows, Q , in each cross-transect. These results were compared with the previous classification of the dynamic of the control volume.

Table 2 shows the characteristics of the control volume and the necessary terms to evaluate the conservation of salinity equation (Eq. 1), calculated from the salinity field data. The

values for the vertical diffusion coefficient for day 1 and day 2 for each cross-transect were selected, taking into account the time the microstructure data were collected. Only the good fits (see Microstructure data) were used to calculate an averaged vertical diffusion coefficient. In some cases, an averaged coef-

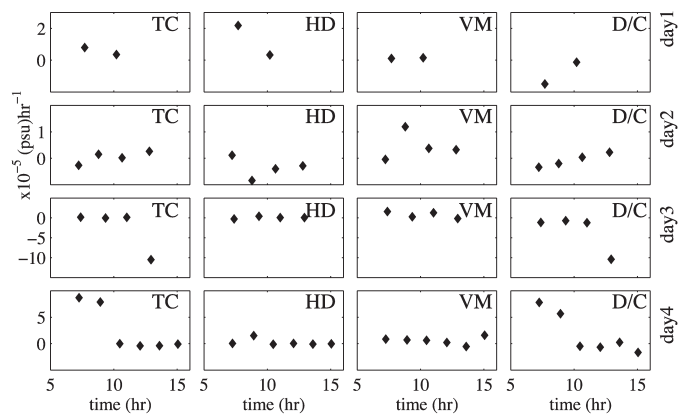


Fig. 5. Fluxes in the conservation of salinity for each day. Positive values represent incoming fluxes due to horizontal diffusion ($\Delta S_{hor\ diff}$; HD), vertical mixing ($\Delta S_{ver\ mix}$; VM), and divergent/convergent fluxes ($\Delta S_{conv/div}$; D/C) that produce the temporal changes of salinity ($\Delta S/\Delta t$; TC) in the control volume.

Table 3. Analysis of the divergent fluxes (Q) and horizontal diffusion coefficient from drogues' movement (k_{hD}) and from salinity mass balance (k_{hS}).

Day*	CT	k_{hD} drogues (m^2s^{-1})	Q (m^3s^{-1})	Dynamic of the CV	k_{hS} mass balance (m^2s^{-1})	Flushing time (hours)	Average sampling interval (hours)	Valid data
1	1	4.8	–	div	1.5	–	2.5	•
	2	4.8	–	div	3.0	–	2.5	•
	3							
2	1	4.9	–1264	loss of ID	–9.7	0.1	1.6	
	2	4.9	22	div	6.1	7.6	1.9	•
	3	4.9	–9	div	4.4	17.9	2.2	•
	4	4.9	–65	conv/div	1.0	2.6	1.7	•
	5							
3	1	4.8	386	div/conv	25.3	0.3	2.0	
	2	4.8	–	div/conv	–3.5		1.7	
	3	4.8	–	div/conv	–64.1		1.9	
	4	4.8	–8353	loss of ID	–583.0	0.02	2.1	
	5							
4	1	1.3	7372	loss of ID	392.4	0.02	1.7	
	2	1.3	92	div/conv	6.2	1.4	1.5	
	3	1.3	108	div/conv	7.0	1.2	1.6	
	4	1.3	–	div/conv	–25.2		1.5	
	5	1.3	–	div/conv	–2.3		1.5	
	6	1.3	1502	div/conv	81.0	0.1	1.5	
	7							

* k_{hS} , salinity mass balance (calculated as [(1) – (3) × (4)]/(2) from Table 2); CT, cross-transects; CV, control volume; $\Delta S_{conv/div}$, calculated as [(1) – (2) × k_{hD} – (3) × (4)] from Table 2; ID, identity.

ficient was calculated including values from the previous or posterior deployments. This was important especially when only one good fit was obtained in a set of deployment. For d 3 and d 4, values from previous days obtained under similar wind conditions were used. The values of the different terms in Eq. 1 for salinity are presented in Fig. 5 where the div/conv flux ($\Delta S_{conv/div}$) represents the term necessary to keep the balance. The daily averaged horizontal diffusion coefficient obtained from the drogues' divergence, k_{hD} , was used in the term $\Delta S_{hor\ diff}$ each day (Table 3). All the fluxes are approximately of the same order of magnitude.

For simplicity and consistency, mean concentrations were calculated below and around the CV, using the averaged horizontal and vertical gradient applied from the center of the CV, respectively, to calculate the advective fluxes (Q). A positive value for Q means a radial flow was coming into the CV, leaving through the bottom. Conversely, a negative value for Q means that a radial flux was leaving the CV through the radial boundary. Due to the simplifications made, it was not possible to obtain a value for Q in all the cases given the signs of the horizontal and vertical gradients. The results from the mass balance equation supported the previous classification of the dynamic of the control volume. Negative values of Q matched the divergence situations, and loss of integrity was associated with high exchange of water. In the case of div/

conv, the value of Q indicates the main effect of the relative movement of the drogues.

For comparison and validation of the previous results and for further analysis, the diffusion coefficient also was calculated from the salinity mass balance, k_{hS} , assuming that $\Delta S_{conv/div} = 0$ (Table 3). These values were consistent with the previous results and showed that they agreed with the dispersion coefficient obtained from the drogues divergence when div/conv fluxes were small and the formation of the drogues kept its integrity.

The aim of the experiment is to ensure that the advective fluxes (div/conv fluxes) are not masking the biological and chemical fluxes. To achieve this, the flushing time or turn over, (volume of CV)/ Q , that indicates the time needed to renew the water in the CV, has to be equal to or larger than the sampling time. Therefore, calculations carried out between two cross-transects with a sampling interval larger than the flushing time were eliminated (Table 3). In d 1, it was assumed that, because of the similar values of horizontal diffusion coefficients obtained from the two analysis (k_{hD} and k_{hS}), the div/conv fluxes were small and the flushing time also was larger than the sampling time.

Residual term $\Delta\Phi_{bio} + \Delta\Phi_{sett}$ —Each term of Eq. 1 was evaluated for DO, Chl a , and the nitrogen species (NH_4 , NO_x , TDN, and TN; Table 4) to find the residual term $\Delta\Phi_{res}$ that would represent the changes due to processes other than hydrodynamic.

Table 4. Terms of the conservation of mass equation (Eq. 1) for dissolved oxygen (DO), chlorophyll *a* (Chl *a*), ammonium (NH₄), nitrate + nitrite (NO_x), total dissolved nitrogen (TDN), and total nitrogen (TN).

Species*	day	CT	Φ	$\Delta\Phi/\Delta t$ [Φ]hr ⁻¹	$\Delta\Phi_{hor\ dif}$ [Φ]hr ⁻¹	$\Delta\Phi_{ver\ mix}$ [Φ]hr ⁻¹	$\Delta\Phi_{res}$ [Φ]hr ⁻¹	
DO (mg L ⁻¹)	1	1	6.19	0.017	0.021	0.004	-0.009	
		2	6.23	0.022	-0.016	-0.013	0.051	
		3	6.29					
	2	2	5.40	0.06	-0.4	0.043	0.41	
		3	5.51	0.36	0.29	0.011	0.06	
		4	6.28	0.06	-0.0029	-0.0097	0.074	
		5	6.38					
	Chl <i>a</i> (μ g L ⁻¹)	1	1	1.2	0.074	0.0025	-0.001	0.072
			2	1.4				
			3					
2		2	2.1	-0.35	0.28	0.23	-0.86	
		3	1.5	0.29	0.31	0.10	-0.11	
		4	2.1	0.68	0.16	0.10	0.42	
		5	3.3					
NH ₄ (μ M N)		1	1	0.5	-0.1	0.02	-0.003	-0.1
			2	0.3	-0.02	0.01	-0.003	-0.07
			3	0.2				
	2	2	0.5	-0.1	0.05	-0.07	-0.07	
		3	0.3	-0.04	0.05	0.0	-0.07	
NO _x (μ M N)	1	1	4.8	-0.86	-0.21	-0.093	-0.5	
		2	3.2	-0.6	-0.1	-0.079	-0.41	
		3	1.8					
	2	2	3.4	0.054	0.011	-0.93	0.93	
		3	3.6	-0.17	0.57	-0.21	-0.54	
TDN (μ M N)	1	1	14.3	-0.66	-0.086	-0.13	-0.45	
		2	12.9	-0.59	-0.36	-0.1	-0.13	
		3	11.4					
	2	2	12.1	-0.16	-0.16	-1.0	1.0	
		3	11.4	-0.065	-0.065	-0.44	0.44	
TN (μ M N)	1	1	15.7	0.15	-0.44	-0.15	0.52	
		2	16.4	-1.3	-2.4	-0.11	0.86	
		3	12.9					
	2	2	15.7	-0.46	0.44	-1.4	0.52	
		3	15.0	-0.52	0.86	-0.43	-0.46	
4	13.6	0.086	0.0035	-0.31	0.29			
5	13.6							

*[Φ], units of concentration of species Φ .

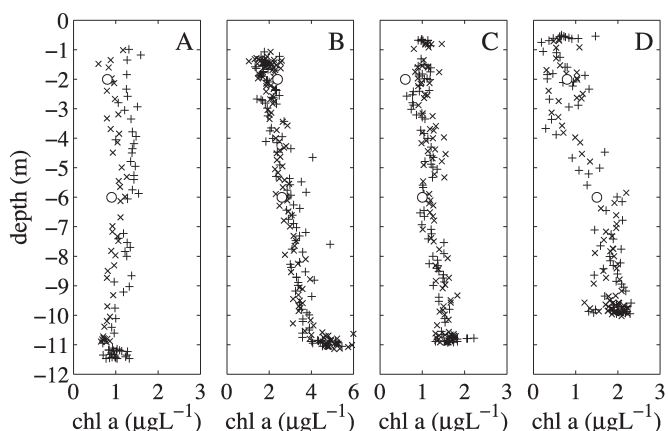


Fig. 6. Comparison between Chl *a* from the fluorescence profiler and Chl *a* from water samples. A) d 3, second cross-transect, B) d 3, fifth cross-transect, C) d 4, second cross-transect, and D) d 4, fourth cross-transect. The symbols + and x represent data from the two probe deployments and the symbol O represents the water samples.

As discussed above, only the valid cases (where the sampling time was smaller than the flushing time) were evaluated. In these cases, the div/convection fluxes were small enough so that both values for diffusion coefficient, k_{hD} (obtained from the drogues' movement) and k_{hS} (obtained from the salinity mass balance with $\Delta S_{conv/div} = 0$) were similar (Table 3). Thus, for the subsequent calculations, the term $\Delta\Phi_{div/conv}$ was disregarded for salinity, and the diffusion coefficients from the salinity calculations (k_{hS}) were used.

The comparison between Chl *a* from the fluorescence profiler and from water samples (Fig. 6) showed a good agreement between both sets of data, following the same trend, validating the use of the probe data as a measure of Chl *a* in this study site. In the case of nitrogen, the mean concentration in the CV, Φ^m , was calculated as the average of the measurements at $z = 2$ m at CD, N3, S3, E3, and W3 in each cross-transect. The net diffusive flux per unit volume ($\Delta\Phi_{hor\ diff}$) for the nitrogen species was estimated as for salinity, DO, and Chl *a*, with the difference that the gradient was calculated between the concentration at N3, S3, E3, and W3 at 2 m depth and the value at CD at 2 m depth. It was assumed that the concentration of all nitrogen variables did not vary in the top meter and thus mixing did not lead to a net flux through the top surface of the CV. The same vertical diffusion coefficient was applied for all the species and the vertical gradient was calculated using the values at 2 m and 6 m depth at CD (Fig. 1). Due to a lack of data, it was assumed that the vertical gradient was 0 for the second and third cross-transect in d 1.

The contribution of the biogeochemical and physical mechanisms to the material change (Fig. 7) showed that they were comparable. This suggested that the experiment effectively captured the residual signal without being overwhelmed by the physical changes. The sampling frequency of hours seemed to have been able to detect changes due to biogeo-

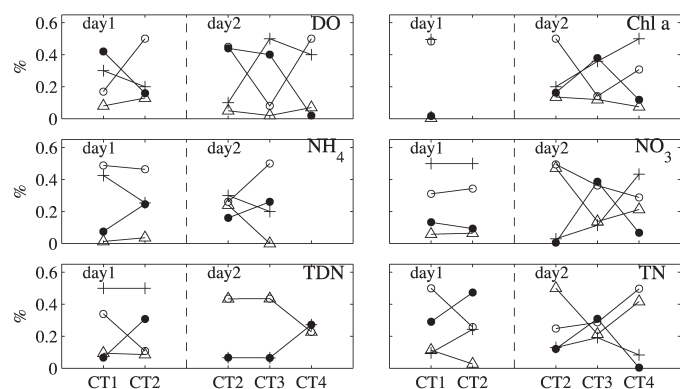


Fig. 7. Percentage of the rates of change of the different processes for DO, Chl *a*, and nitrogen species. The 100% corresponds to the sum of the absolute values of $|\Delta\Phi/\Delta t| + |\Delta\Phi_{hor\ diff}| + |\Delta\Phi_{vert\ mix}| + |\Delta\Phi_{res}|$. The symbol + represents the material change, ● represents the horizontal diffusion, △ represents vertical mixing, and ○ represents biogeochemical processes and settling.

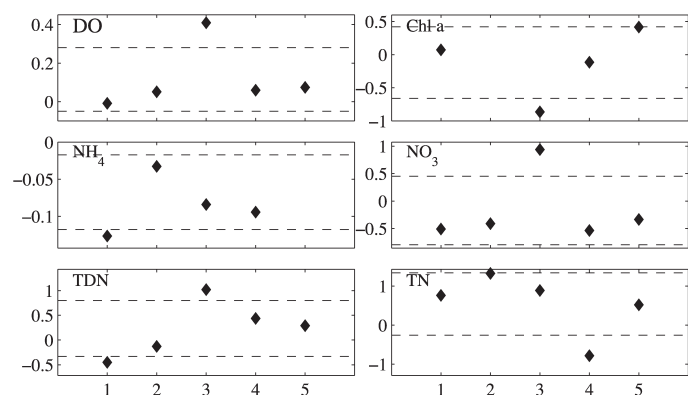


Fig. 8. Estimate of residual terms of DO ($\text{mg O}_2 \text{ L}^{-1} \text{ hr}^{-1}$), Chl *a* ($\mu\text{g Chl } a \text{ L}^{-1} \text{ hr}^{-1}$), NH_4 ($\mu\text{moles N L}^{-1} \text{ hr}^{-1}$), NO_x ($\mu\text{moles N L}^{-1} \text{ hr}^{-1}$), TDN ($\mu\text{moles N L}^{-1} \text{ hr}^{-1}$), and F) TN ($\mu\text{moles N L}^{-1} \text{ hr}^{-1}$).

chemical processes. This implies that sampling time scales were of the order of the characteristic scales for the internal cycling rates. The contribution of horizontal dispersion and vertical mixing to the changes in the concentration of biological and chemical species was quantified by using sampling scales similar to the time scales of these processes. In this study, the horizontal and vertical length scales of interest were of the order of ~ 100 meters and 1 meter respectively. Diffusion time scales, calculated as L^2/k where L is a length scale and k is the diffusion coefficient, yielded values of the order of hours. In the case of the divergent and convergent fluxes, their interference was removed by assuring that the sampling scales and the biogeochemical scales were smaller than the flushing time. Thus, the results and this analysis also suggested that the scales chosen for the experiment were appropriate.

A statistical analysis was not performed due to the limited amount of data obtained after the validation. Instead, a sim-

ple criterion was applied to the residual terms to eliminate the extreme values. A region was defined with limits set as the mean value \pm standard deviation (Fig. 8) and only the values within this region were considered subsequently. If two points were outside this region but in opposite extremes, these points were not eliminated. After this analysis, the mean value and the standard deviation (SD) for the remaining residual terms were: $\Delta(\text{DO})_{res} = 0.04 \mu\text{g O}_2 \text{ L}^{-1} \text{ hr}^{-1}$ (SD = 0.04), $\Delta(\text{Chl } a)_{res} = 0.1 \mu\text{g Chl } a \text{ L}^{-1} \text{ hr}^{-1}$ (SD = 0.3), and $\Delta(\text{NH}_4)_{res} = -0.07 \mu\text{moles N L}^{-1} \text{ hr}^{-1}$ (SD = 0.05), $\Delta(\text{NO}_x)_{res} = -0.45 \mu\text{moles N L}^{-1} \text{ hr}^{-1}$ (SD = 0.09), $\Delta(\text{TDN})_{res} = 0.2 \mu\text{moles N L}^{-1} \text{ hr}^{-1}$ (SD = 0.6), and $\Delta(\text{TN})_{res} = 0.9 \mu\text{moles N L}^{-1} \text{ hr}^{-1}$ (SD = 0.3).

The resulting residual terms presented high variability. The factors that could be identified to explain this variability are: diurnal variations (Lorenzen 1963), limited amount of valid data for the final analysis (Table 3), sampling frequency, and methods of analysis. For instance, if the sampling resolution was larger than the scales of patterns, then the sampling strategy was not able to capture the spatial variability of the species concentration, leading to inaccuracies in the determination of the fluxes and concentration in the control volume. This argument could be more important in the case of nitrogen as the sampling frequency was much lower than for DO and Chl *a*.

Validation of the internal biogeochemical rates—The net growth rate was calculated as the production rate/biomass ratio (Kirchman 2002, Marañon 2005) in terms of Chl *a*, i.e., $(\Delta(\text{Chl } a)_{bio} / \text{Chl } a)$ where $\Delta(\text{Chl } a)_{bio}$ is the net change due to mortality, growth, and grazing. The net change in Chl *a* due to biogeochemical processes is given by $\Delta(\text{Chl } a)_{bio} = \Delta(\text{Chl } a)_{res} - \Delta(\text{Chl } a)_{sett}$ (Table 5, Eq. 19). The fluxes due to settling were calculated as $(\Phi_T - \Phi_B) \nu_s A/V$ with Φ_T and Φ_B the species concentration at the top and bottom of the control volume, respectively, ν_s the settling velocity and A and V the bottom area and volume of the control volume, respectively. With a mean value for $(\Phi_T - \Phi_B)$ for Chl *a* (for the valid cross-transsects) equal to $-0.18 \mu\text{g (Chl } a) \text{ L}^{-1}$ and a settling velocity in the range of 0.2 md^{-1} and 2 md^{-1} (Jorgensen et al. 1991 and references therein, Wetzel 2001 and references therein), then $\Delta(\text{Chl } a)_{sett}$ ranged between 5×10^{-4} and $5 \times 10^{-3} \mu\text{g (Chl } a) \text{ L}^{-1} \text{ hr}^{-1}$. With a mean value for Chl *a* equal to $1.9 \mu\text{g (Chl } a) \text{ L}^{-1}$, the value obtained for the net growth rate varied between 1.4 and 1.5 d^{-1} , which is within the range found in literature (Jorgensen et al. 1991 and references therein).

In addition to growth rate, primary production, C:Chl *a* and nitrogen transformation rates were estimated to further assess the approach used in this study and the validity of the internal rates. Primary production was calculated using the net production of oxygen obtained from the experiment, $\Delta(\text{DO})_{res}$, that was the result of photosynthesis and respiration of organisms and microbial processes. For these calculations, however, it was assumed that, as a first approximation, the effect of organisms other than phytoplankton could be disregarded (Table 5).

CO_2 and dissolved nutrients are used in photosynthesis and other metabolic pathways to synthesize many of the com-

Table 5. Processes affecting the rate of change of nitrogen, DO, and Chl *a*. Zooplankton and microbial contribution to the mass balance have been disregarded.

1)	$\Delta(\text{TN})_{res}$	=	$\Delta(\text{TDN})_{res}$	$+\Delta(\text{TPN})_{res}$	$+\Delta(\text{IN})_{res}$		
2)	$\Delta(\text{TDN})_{res}$	=	$\Delta(\text{DIN})_{res}$	$+\Delta(\text{DON})_{res}$			
3)	$\Delta(\text{TPN})_{res}$	=	$\Delta(\text{PIN})_{res}$	$+\Delta(\text{PON})_{res}$			
4)	$\Delta(\text{DON})_{res}$	=	$\Delta(\text{DON})_{dec}$	$+\Delta(\text{DON})_{min}$	$+\Delta(\text{DON})_{mor/exc}$		
5)	$\Delta(\text{PIN})_{res}$	=	$\Delta(\text{PIN})_{ad/de}$	$+\Delta(\text{PIN})_{sett}$			
6)	$\Delta(\text{PON})_{res}$	=	$\Delta(\text{PON})_{dec}$	$+\Delta(\text{PON})_{mor/exc}$	$+\Delta(\text{PON})_{sett}$		
7)	$\Delta(\text{IN})_{res}$	=	$\Delta(\text{IN})_{upt\ NH_4}$	$+\Delta(\text{IN})_{upt\ NO_3}$	$+\Delta(\text{IN})_{sett}$	$+\Delta(\text{IN})_{mor/exc}$	$+\Delta(\text{IN})_{fix}$
8)	$\Delta(\text{DIN})_{res}$	=	$\Delta(\text{NH}_4)_{res}$	$+\Delta(\text{NO}_3)_{res}$			
9)	$\Delta(\text{NH}_4)_{res}$	=	$\Delta(\text{NH}_4)_{min}$	$+\Delta(\text{NH}_4)_{ad/de}$	$+\Delta(\text{NH}_4)_{upt}$	$+\Delta(\text{NH}_4)_{nitrif}$	
10)	$\Delta(\text{NO}_x)_{res}$	=	$\Delta(\text{NO}_3)_{nitrif}$	$+\Delta(\text{NO}_3)_{upt}$	$+\Delta(\text{NO}_3)_{den}$		
11)	$\Delta(\text{NH}_4)_{min}$	=	$-\Delta(\text{DON})_{min}$				
12)	$\Delta(\text{NH}_4)_{upt}$	=	$-\Delta(\text{IN})_{upt\ NH_4}$				
13)	$\Delta(\text{NH}_4)_{ad/de}$	=	$-\Delta(\text{PIN})_{ad/de}$				
14)	$\Delta(\text{NH}_4)_{nitrif}$	=	$-\Delta(\text{NO}_3)_{nitrif}$				
15)	$\Delta(\text{NO}_3)_{upt}$	=	$-\Delta(\text{IN})_{upt\ NO_3}$				
16)	$\Delta(\text{DON})_{dec}$	=	$-\Delta(\text{PON})_{dec}$				
17)	$\Delta(\text{IN})_{mor/exc}$	=	$-\Delta(\text{DON})_{mor/exc}$	$-\Delta(\text{PON})_{mor/exc}$			
18)	$\Delta(\text{DO})_{res}$	=	$\Delta(\text{DO})_{bac}$	$+\Delta(\text{DO})_{nitrif}$	$+\Delta(\text{DO})_{phot}$	$+\Delta(\text{DO})_{resp}$	
19)	$\Delta(\text{Chl } a)_{res}$	=	$\Delta(\text{Chl } a)_{grow}$	$+\Delta(\text{Chl } a)_{mor/exc}$	$+\Delta(\text{Chl } a)_{sett}$		
0	<		$\Delta(\text{NH}_4)_{min}, \Delta(\text{NO}_3)_{nitrif}, \Delta(\text{DON})_{dec}, \Delta(\text{DON})_{mor/exc}, \Delta(\text{PON})_{mor/exc}, \Delta(\text{IN})_{fix}$				
0	>		$+\Delta(\text{NH}_4)_{upt}, +\Delta(\text{NO}_3)_{upt}, \Delta(\text{PIN})_{sett}, \Delta(\text{PON})_{sett}$				

*TN, total nitrogen; TDN, total dissolved nitrogen; TPN, total particulate nitrogen; IN, inorganic nitrogen; DIN, dissolved inorganic nitrogen; DON, dissolved organic nitrogen; PIN, particulate inorganic nitrogen; PON, particulate organic nitrogen; NH₄, ammonium; NO₃, nitrate; NO_x, nitrate + nitrite; DO, dissolved oxygen; Chl *a*, chlorophyll *a*; N, nitrogen; subscript *res*, residual term $\Delta\Phi_{bio} + \Delta\Phi_{sett}$; subscript *dec*, decomposition of particulate organic nitrogen; subscript *min*, mineralization of dissolved organic nitrogen; subscript *mor/exc*, phytoplankton mortality and excretion; subscript *ad/de*, adsorption/desorption of NH₄ onto inorganic suspended solids or particulate inorganic nitrogen; subscript *sett*, settling; subscript *upt*, phytoplankton uptake of NH₄ and NO_x; subscript *fix*, nitrogen fixation; subscript *nitrif*, nitrification; subscript *den*, denitrification; subscript *bac*, the action of bacteria on organic matter; subscript *phot*, photosynthesis; subscript *resp*, respiration; and subscript *grow*, phytoplankton growth.

pounds present in the phytoplankton cells (fats, proteins, and organic acids). In this process, biomass or organic matter increases and dissolved oxygen is released. Ryther (1956) concluded that values for the photosynthetic quotient (PQ), defined as the ratio of oxygen produced to carbon dioxide assimilated, between 1.1 and 1.3 or higher are normal in natural conditions, suggesting a value of 1.25. Also, comparisons between the O₂ and the ¹⁴C techniques revealed, generally, a

Table 6. Daily averaged values in the control volume.

Φ	unit	day 1	day 2	day 3	day 4
Chl <i>a</i>	μg L ⁻¹	1.3	2.3	1.6	1.4
DO	mg L ⁻¹	6.3	6.0	6.4	6.8
NH ₄	μmoles N L ⁻¹	0.3	0.4	0.3	0.4
NO ₃	μmoles N L ⁻¹	3.3	3.1	2.1	3.3
TDN	μmoles N L ⁻¹	13.4	11.8	10.4	12.2
TN	μmoles N L ⁻¹	16.0	14.4	13.4	14.1
DON	μmoles N L ⁻¹	9.1	8.4	7.9	8.5
TPN	μmoles N L ⁻¹	2.4	2.5	3.1	1.9

Φ , species; Chl *a*, chlorophyll *a*; DO, dissolved oxygen; NH₄, ammonium; NO₃, nitrate; TDN, total dissolved nitrogen; TN, total nitrogen; DON, dissolved organic nitrogen; and TPN, total particulate nitrogen.

good agreement if a value of PQ = 1.2 is used (Harris 1980). In many situations however, the ¹⁴C method has yielded a measure rather close to the net photosynthetic rates; in those cases ¹⁴C uptake was close to the net oxygen production when a value of PQ = 1.25 was used (Ryther 1956). In this study, net primary production was estimated by calculating a carbon equivalent to the rate of change of DO, using the residual term ΔDO_{res} and a value of PQ = 1.25. It was assumed that this rate of change of the internal carbon in phytoplankton corresponded to a net uptake due to assimilation and losses.

The positive values obtained for the DO and Chl *a* residual terms did not contradict the assumption of primary production being the prevailing mechanism affecting those species. With this assumption, the amount of net carbon uptake was 12 μg C L⁻¹hr⁻¹. Thompson and Waite (2003) obtained similar values for the maximum carbon fixation in the area. Assuming that phytoplankton response to the nutrient supply was not as fast as the sampling frequency and duration of the experiment (Duarte 1990), and that light exposure varied gradually, then it was possible to accept the balanced growth condition. A balanced growth implies that the specific rate of changes of indices of biomass such as C, N, and Chl *a* are equal (Eppley, 1980) i.e., $\Delta C/C = \Delta N/N = \Delta \text{Chl } a/\text{Chl } a$, and

processes of carbon assimilation, nutrient uptake, and chlorophyll production are coupled. If balanced growth is assumed, the carbon to Chl *a* ratio, estimated from the change of internal carbon or net uptake and $\Delta(\text{Chl}a)_{\text{bio}}$ ($C:\text{Chl}a = \Delta C / \Delta(\text{Chl}a)_{\text{bio}}$) is ~ 102 .

Cell counts showed, as in previous studies, that Bacillariophyceae (diatoms) was the dominant phytoplankton group during the field study and comprised 51%–95% of the population. Studies carried out with healthy and nutrient-sufficient cells of diatoms have yielded values for C:Chl *a* ranging between 21.5 and 46.6 mg C (mg Chl *a*)⁻¹ (Gallegos and Vant 1996) although double or even higher values also have been reported (Jorgensen et al. 1991 and references therein). C:Chl *a* has been found to depend on the physiological response of the phytoplankton to environmental fluctuations, i.e., nutrient supply and light, varying in a considerable range. For nitrogen-limited and starved diatoms cultures, values ranged from 22 up to 155 mg C (mg Chl *a*)⁻¹ (Jorgensen et al. 1991 and references therein) have been reported. Wetzel (2001) presented limits for C:Chl *a* for nutrient limited phytoplankton in the range of 50 to 100 for moderate cases and >100 for severe limitation. The C:Chl *a* obtained in this experiment, where phytoplankton are nitrogen limited as mentioned before, agreed with these values for nutrient limited phytoplankton.

The processes involved in the nitrogen dynamic are summarized in Table 6, where zooplankton and microbial contribution to the mass balance have been disregarded as mentioned before, as a first approximation. To verify the accuracy of the nitrogen residual terms obtained from the experiment, a comparison between these data and literature values was performed. Processes such as adsorption and desorption were disregarded due to the low concentrations of particles such as sand and other inert species (turbidity values were below 5 FTU during the 4-d experiment.). Also nitrogen fixation was disregarded due to the characteristics of the study site: low concentrations or absence of cyanobacteria (Cyanophyceae was only found in one sample with less than 1% of the total cell count), and high degree of turbulence that inhibits the formation of microzones. These microzones favor nitrogen fixation as nitrogenase is oxygen-sensitive (Howarth et al. 1988 and references therein). As for nitrogen fixation, denitrification also was disregarded due to high concentration of DO (~ 6.0 mgL⁻¹, Table 6); an oxygen concentration of <0.2 mg L⁻¹ is required for denitrification (Seitzinger 1988).

Under the balanced growth assumption, Chl *a* was converted to phytoplankton content of nitrogen ($IN = 0.950$ $\mu\text{moles N L}^{-1}$) by using the ratio C:Chl *a* obtained above and by assuming a phytoplankton molar C:N ratio equal to 14.6. Limits for C:N for nitrogen limited phytoplankton in the range of 8.3 to 14.6 (molar) can be found for moderate cases and >14.6 for severe limitation (Wetzel 2001). Redfield ratio is C:N = 6.6 (Redfield et al. 1963). Under the same assumption ($\Delta IN / IN = \Delta(\text{Chl}a)_{\text{bio}} / \text{Chl}a = \Delta C / C$), the net change of internal nitrogen due only to uptake and losses yielded a value of $\Delta(IN)$

$$= \Delta(IN)_{\text{upt NH}_4} + \Delta(IN)_{\text{upte NO}_3} + \Delta(IN)_{\text{mor/exc}} = 0.059 \mu\text{moles N L}^{-1} \text{ hr}^{-1} \text{ (see Eq. 7, Table 5).}$$

The sources and sinks for TN can be rewritten as $\Delta(TN)_{\text{res}} = \Delta(POM)_{\text{sett}} + \Delta(IN)_{\text{sett}} + \Delta(IN)_{\text{fix}} + \Delta(NO_3)_{\text{den}}$ by combining Eq. 1–17 (Table 5). The mean value for $(\Phi_T - \Phi_B)$ for particulate nitrogen (TPN) considering only detrital nitrogen, showed an average of 0.48 $\mu\text{moles N L}^{-1}$. Assuming a settling velocity for particulate matter of between 0.2 and 2 md⁻¹, the fluxes per unit volume due to settling are $\Delta(POM)_{\text{sett}} \sim 0.016$ $\mu\text{moles N L}^{-1} \text{ hr}^{-1}$. $\Delta(IN)_{\text{sett}} = -0.0011$ $\mu\text{moles N L}^{-1} \text{ hr}^{-1}$ with $(\Phi_T - \Phi_B)$ equal to 0.02 $\mu\text{moles N L}^{-1}$. And with the previous assumptions of $\Delta(IN)_{\text{fix}} \approx 0$ and $\Delta(NO_3)_{\text{den}} \approx 0$, $\Delta(TN)_{\text{res}}$ yielded a value of +0.010 $\mu\text{moles N L}^{-1} \text{ hr}^{-1}$. This figure is two orders of magnitude smaller than the value found for $\Delta(TN)_{\text{res}}$ from this experiment (see previous section).

Using a mortality rate equal to $k_M = 0.004$ hr⁻¹ (Jorgensen 1991), $\Delta(IN)_{\text{mor/exc}} = (IN k_M) = -0.004$ $\mu\text{moles N L}^{-1} \text{ hr}^{-1}$ and $\Delta(IN)_{\text{uptake NH}_4} + \Delta(IN)_{\text{uptake NO}_3} = \Delta(IN) - \Delta(IN)_{\text{mor/exc}} = 0.055$ $\mu\text{moles N L}^{-1} \text{ hr}^{-1}$. Rates for decomposition of the labile dissolved organic matter (\sim assumed to be 90% of the dissolved organic matter, DOM) range between 2–3% in 6 d (Wetzel 2001 and reference therein). Assuming a value of 8%, and calculating the dissolved organic nitrogen, DON, equal to TDN – DIN (DIN, dissolved inorganic nitrogen, = $\text{NO}_3 + \text{NH}_4$), $\Delta(DON)_{\text{mineral}} = -\Delta(\text{NH}_4)_{\text{mineral}} = -0.004$ $\mu\text{moles N L}^{-1} \text{ hr}^{-1}$. As $\Delta(\text{NH}_4)_{\text{uptake}} + \Delta(\text{NO}_3)_{\text{uptake}} = -0.055$ $\mu\text{moles N L}^{-1} \text{ hr}^{-1}$ then $\Delta(\text{NH}_4)_{\text{res}} + \Delta(\text{NO}_3)_{\text{res}} = -0.051$ $\mu\text{moles N L}^{-1} \text{ hr}^{-1}$ (combining Eq. 9, 10, and 14, Table 6) that is smaller than the value yielded by this experiment. Values of organic matter decomposition showed that 5–35% of the total biomass is released as DOM (Wetzel 2001). Assuming 20% is released in the form of DOM and 80% in the form of POM, $\Delta(DON)_{\text{mor/exc}} = 0.01$ $\mu\text{moles N L}^{-1} \text{ hr}^{-1}$ and $\Delta(POM)_{\text{mor/exc}} = 0.06$ $\mu\text{moles N L}^{-1} \text{ hr}^{-1}$. A rate of decomposition of particulate nitrogen of 10% per day was assumed (Wetzel 2001) yielding $\Delta(POM)_{\text{dec}} = -0.007$ $\mu\text{moles N L}^{-1} \text{ hr}^{-1}$ and a $\Delta(POM)_{\text{res}} = 0.040$ $\mu\text{moles N L}^{-1} \text{ hr}^{-1}$. From Eq. 1 and 3 in Table 6, $\Delta(TDN)_{\text{res}} = -0.096$ $\mu\text{moles N L}^{-1} \text{ hr}^{-1}$.

Results yielded growth rates and primary production within literature values although they appeared to be in the upper limit given the characteristics of the area. This study site presents a high degree of nitrogen limitation that was reflected in the high value of C:Chl *a* obtained from the experiment. In the case of primary productivity, the value could have been underestimated since the net oxygen change due only to phytoplankton should then be higher if the effect of respiration of organisms in other different trophic levels is not disregarded. In contrast to the rates of processes obtained for phytoplankton, the internal changes for nitrogen obtained from the experiment showed low correspondence with values observed in other studies, with differences of the order of magnitude up to 2.

Due to the relevance of the accuracy of the estimates of fluxes, especially in oligotrophic systems, it is convenient to undertake a preliminary analysis of some of the factors that could affect the results presented. In the calculation of the

processes of nitrogen, the possible sources of inaccuracies could be found in the spatial sampling resolution, as stated before, and in the method of analysis, as shown in the latter calculations. In this case, the direct chemical measurements used for the analysis do not seem to have been sufficiently sensitive given the very low concentration of phytoplankton and nutrient in the study area (Table 6), and the sampling time.

In the case of DO and Chl *a* measurements (used to calculate growth rates, primary production and C:Chl *a*) the possible sources of variability could be more associated with diurnal variations and the limited amount of valid data for the analysis. In terms of precision of instruments used to measure DO, it seems to have been adequate given the characteristics of the study area (Carignan 1998). Issues with the accuracy of the instrument could be acceptable if one considers that all the calculations for DO imply a difference between two measurements, where any differences from the real value could be compensated. In the case of the use of *in situ* fluorescence as an index of Chl *a*, the results need to be used with caution due to the different factors that affect the relationship between these variables (Kiefer et al. 1989; Kolber and Falkowski 1993). This implies that changes in the fluorescence yield are not necessarily related to changes in phytoplankton biomass or Chl *a* content. In the analysis undertaken in this study, as in the case of DO, the relevant estimate is the difference between Chl *a* values more than the absolute value. Although the use of *in situ* fluorescence needs to be considered as a source of inaccuracy, it could be stated that the data processing could then partly compensate for the error associated with each Chl *a* result. This could be accepted, for instance, if it is assumed that the ambient light intensity is considered relatively constant between two cross-transects.

Additionally, it could be important to analyze the accuracy in the calculation of vertical fluxes. Some errors could come from the assumptions made about the value of the mixing efficiency, R_f . For instance, a decrease of 40% in the R_f value used produces a decrease of 28% in the vertical coefficient and in turn in the vertical fluxes. Other errors could be generated by an inadequate amount of valid data from the microstructure profiler to estimate the vertical diffusion coefficient (some data did not present a good fit, and thus a number higher than five deployments after each cross-transect sampling could have been more appropriate). The effect of these sources of inaccuracies on the residual term of DO and Chl *a* was analyzed. It was found that a 2% change in the DO residual term appears associated with a 50% increase or decrease in the DO vertical fluxes, with an increase of 4% if the vertical fluxes increase 100%. In the case of the Chl *a*, a change in the vertical fluxes of 50% generates a change in the Chl *a* residual term of 27%, with a decrease of 53% if the vertical fluxes increase 100%. With these results, it is possible to see that the results derived from DO calculations should not be affected by errors in the vertical flux determinations. In the case of the growth rate and C/Chl *a* ratio, the values obtained could

increase or decrease according to the changes of the Chl *a* residual term.

The results for the biogeochemical rates and physiological conditions were subject to some potential sources of inaccuracies present in the experiment and in the assumptions made based on results from other studies. In spite of this, the fact that growth rates, primary production, and C:Chl *a* were within reasonable values supported the validity of the experiment. It also highlights the advantage of the experiment in providing *in situ* information at scales of hours in systems with high complexity due to hydrodynamic and heterogeneity in species concentration.

Discussion

The Lagrangian approach provides an adequate means of estimating biogeochemical changes *in situ*, maintaining the natural conditions of critical factors in the response of phytoplankton such as mixing depth, turbulence, light, and nutrient availability. With this method, rates of biogeochemical processes can be estimated at scales of hours, providing an insight into the details of the dynamic of the ecosystem. This information normally is missed in field experiments that used scales of weeks or months and can be found only in laboratory studies, where the natural conditions have been greatly altered.

A key point in this approach is that the quantification of internal rates is undergone by effectively isolating the biogeochemical-induced changes from both the advective and diffusive interference. An accurate quantification of advective fluxes is difficult to achieve if the sampling design is not able to capture the variability in the velocity field and concentration of the species of interest. The difference from other methods is that this issue is addressed by removing the interference of the unaccounted advective fluxes in the measured changes of concentration. In this way, the errors associated with the quantification of the advective fluxes were minimized.

The experiment design presents a critical aspect. This is given by the relationship between the time scales of advection (T_A), diffusion (T_D), biogeochemical processes (T_R), and the sampling (T_S). To assure that biogeochemical processes are not overwhelmed by the physical processes then $T_R \leq T_A, T_D$. In turn, to capture the variability due to the internal processes, T_S has to be equal to or smaller than T_R , but long enough to detect the changes. In fact it can be $T_S \sim T_R$. Thus, the design of the sampling strategy is subject to this hierarchy of the time scales to successfully isolate the biogeochemical-induced changes from the effect of transport and mixing processes.

The key point in the design of the experiment is to fulfill the relationship $V/Q > T_R \sim T_S$, where V is the control volume and Q the mass flow across the control volume. This relationship establishes that the size of the control volume has to be large enough for the flushing time to be longer than the time scale of the internal process in the control volume. Hence, the concentration changes in the control volume are dominated

by the local cycling within the control volume and are not going to be masked by the external advective fluxes. This relationship can be expressed as $L > \nu T_{R'} \sim \nu T_s$, where L is a length scale characterizing the size of the control volume and ν is the characteristic velocity of the conv/div flows. In addition, the flushing time has to be longer than the sampling time, and thus, there must be a compromise between the size of control volume and the sampling strategy.

To fulfill the previous relationships, it is necessary to consider the factors that affect T_s and $T_{R'}$. The sampling time scale, T_s , depends on the number of sampling stations and the amount of data collected in each station. The number of sampling stations has to consider the scales of patchiness. And, the diffusion time scale depends on the scales of the study and the diffusion coefficient.

References

- Broenkow, W. W. 1965. The distribution of nutrients in the Costa Rica dome in the eastern tropical Pacific Ocean. *Limnol. Oceanogr.* 10:40–52.
- Caraco, N. F., J. J. Cole, and G. E. Likens. 1992. New and recycled primary production in an oligotrophic lake: Insights for summer phosphorus dynamics. *Limnol. Oceanogr.* 37: 590–602.
- Carignan, R. 1998. Automated determination of carbon dioxide, oxygen, and nitrogen partial pressures in surface waters. *Limnol. Oceanogr.* 43:969–975.
- Coale, K. H., K. S. Johnson, S. E. Fitzwater, S. P. G. Blain, T. P. Stanton, and T. L. Coley. 1998. IronEx-I, an *in situ* iron-enrichment experiment: Experimental design, implementation and results. *Deep-Sea Research II* 45:919–945.
- Cole, J. J., M. L. Pace, S. R. Carpenter, and J. F. Kitchell. 2000. Persistence of net heterotrophy in lakes during nutrient addition and food web manipulations. *Limnol. Oceanogr.* 45:1718–1730.
- D'Avanzo, C., J. W. Kremer, and S. C. Wainright. 1995. Ecosystem production and respiration in response to eutrophication in shallow temperature estuaries. *Mar. Ecol. Progr. Ser.* 69:51–54.
- Dortch, Q., and J. R. Postel. 1989. Biochemical indicators of N utilization by phytoplankton during upwelling off the Washington coast. *Limnol. Oceanogr.* 34:738–773.
- Duarte, C. M. 1990. Time lags in algal growth: generality, causes, and consequences. *Journal of Plankton Research.* 12:873–883.
- Dutilleul, P. 1993. Spatial heterogeneity and the design of ecological field experiment. *Ecology.* 74:1646–1658.
- Eppley, R. W., J. N. Rogers, and J. J. McCarthy. 1969. Half-saturation constants for uptake of nitrate and ammonium by marine phytoplankton. *Limnol. Oceanogr.* 14:912–920.
- Fischer, H. B., E. J. List, R. C. Y. Koh, J. Imberger, and N. H. Brooks. 1979. Mixing in inland and coastal waters. Academic.
- Gallegos C. L. and W. N. Vant. 1996. An incubation procedure for estimating carbon-to-chlorophyll ratios and growth-irradiance relationships of estuarine phytoplankton. *Mar. Ecol. Progr. Ser.* 38:275–291.
- Genin, A., G. Yahel, M. A. Reidenbach, S. G. Monismith, and J. R. Koseff. 2002. Intense benthic grazing on phytoplankton in coral reefs revealed using the control volume approach. *Oceanography* 15:90–96.
- Greenberg, A. E., L. S. Clesceri, and A. D. Eaton [Eds.]. 1992. Standard methods for the examination of water and wastewater. American Public Health Association.
- Gribsholt, B., and others. 2005. Nitrogen processing in a tidal freshwater marsh: a whole-ecosystem ^{15}N labeling study. *Limnol. Oceanogr.* 50:1945–1959.
- Harris, G.P. 1980. The measurement of photosynthesis in natural populations of phytoplankton, p: 129–187. *In* I. Morris [Eds.], *The physiological ecology of phytoplankton*. University of California Press, California.
- Hillmer, I., and J. Imberger. 2007 Influence of advection on scales of ecological studies in a coastal equilibrium flow. *Continental Shelf Research* 27:134–153.
- Howarth, R. W., R. Marino, and J. Lane. 1988. Nitrogen fixation in freshwater, estuarine, and marine ecosystems. 1. Rates and importance. *Limnol. Oceanogr.* 33: 669–687.
- Imberger, J., T. Berman, R. R. Christian, E. B. Sherr, D. E. Whitney, L. R. Pomeroy, R. G. Wiegert, and W. J. Wiebe. 1983. The influence of water motion on the distribution and transport of materials in a salt marsh estuary. *Limnol. Oceanogr.* 28:201–214.
- Imberger, J., and G. N. Ivey. 1991. On the nature of turbulence in stratified fluid. Part II: Application to lakes. *Journal of Physical Oceanography.* 21:659–679.
- Ivey, G. N., and J. Imberger. 1991. On the nature of turbulence in stratified fluid. Part I: The energetics of mixing. *Journal of Physical Oceanography.* 21:650–658.
- Johnson, K. S. 1983. Determination of nitrate and nitrite in seawater by flow injection analysis with injection of reagent. *Limnol. Oceanogr.* 28:1260–1266.
- Johannes, R. E., and C. J. Hearn. 1985. The effect of submarine groundwater discharge on nutrient and salinity regimes in a coastal lagoon of Perth, Western Australia. *Estuarine, Coastal and Shelf Science.* 21:789–800.
- Jorgensen, S. E., S. N. Nielsen, and L. A. Jorgensen. 1991. *Handbook of ecological parameters and ecotoxicology*. Elsevier, Amsterdam.
- Ketchum, B. H., and N. Corwin. 1965. The cycle of phosphorus in a plankton bloom in the Gulf of Maine. *Limnol. Oceanogr.* 10:148–161.
- Kiefer, D. A., W. S. Chamberlin, and C. R. Booth. 1989. Natural fluorescence of chlorophyll *a*: Relationship to photosynthesis and chlorophyll concentration in the western South Pacific gyre. *Limnol. Oceanogr.* 34:868–881.
- Kirchman, D. L. 2002. Calculating microbial growth rates from data on production and standing stocks. *Mar. Ecol. Progr. Ser.* 233:303–306.

- Kraines, S., Y. Suzuki, K. Yamada, and H. Komiyama. 1996. Separating biological and physical changes in dissolved oxygen concentration in a coral reef. *Limnol. Oceanogr.* 41:1790–1799.
- Kolber, Z., and P. G. Falkowski. 1993. Use of active fluorescence to estimate phytoplankton photosynthesis *in situ*. *Limnol. Oceanogr.* 38:1646–1665.
- Lord, D. A. 2000. Perth long-term Ocean Outlet Monitoring (PLOOM) programme. 1995-2000; Summary Report. The Water Corporation.
- Lorenzen, J. 1963. Diurnal variations in photosynthetic activity of natural phytoplankton populations. *Limnol. Oceanogr.* 8:56–62.
- Luketina, D. A., and J. Imberger. 2001. Determining turbulent kinetic energy dissipation from the Batchelor curve fitting. *Journal of atmospheric and oceanic technology.* 18: 100–113.
- Marañón, E. 2005. Phytoplankton growth rates in the Atlantic subtropical. *Limnol. Oceanogr.* 50:299–310.
- Marra, J. 1978*a*. Effect of short-term variations in light intensity on photosynthesis of a marine phytoplankton: a laboratory simulation study. *Marine Biology* 46:191–202.
- — —. 1978*b*. Phytoplankton photosynthetic response to vertical movement in mixed layer. *Marine Biology* 46: 203–208.
- — —. 1980. Vertical mixing and primary production, p. 121–137. *In* P.G. Falkowski [Ed.], *Primary productivity in the sea*. Plenum Publishing Corp.
- Melack, J.M. 1982. Photosynthetic activity and respiration in an equatorial African Soda Lake. *Freshwat. Biol.* 12: 381–399.
- Minas, H. J., M. Minas, and T. T. Packard. 1986. Productivity in upwelling areas deduced from hydrographic and chemical fields. *Limnol. Oceanogr.* 31:1182–1206.
- Odum, H. T. 1956. Primary production in flowing waters. *Limnol. Oceanogr.* 1:102–117.
- Osborn, T. R. 1980. Estimates of the rate of the vertical diffusion from dissipation measurements. *J. Phys. Oceanogr.* 10: 83–89.
- Pace, M.L., and J.J. Cole. 1996. Regulation of bacteria by resources and predation tested in whole-lake experiments. *Limnol. Oceanogr.* 41:1448–1460.
- Park, G., and others. 2005. A sulfur hexafluoride-based Lagrangian study on initiation and accumulation of the red tide *Cochlodinium polykrikoides* in southern coastal waters of Korea. *Limnol. Oceanogr.* 50:578–586.
- Pattiaratchi, C.B., and C. Knock. 1995. Perth coastal waters study. Physical measurements. Project P2. Report to Water Authority of Western Australia. University of Western Australia.
- Platt, T., and K.L. Denman. 1975. Spectral analysis in ecology. *Annual Review of Ecology and Systematics.* 6:189–210.
- Redfield, B., H. Ketchum, and F.A. Richards. 1963. The influence of organisms on the composition of sea-water, p. 26–77. *In* M. N. Hill, E. D. Goldberg, C. O'D. Iselin, and W. H. Munk [Eds.], *The Sea*. Interscience.
- Ryther, J. H. 1956. The measurement of primary production. *Limnol. Oceanogr.* 1:72–84.
- Sietzinger, S. 1988. Denitrification in freshwater and coastal marine ecosystems: ecological and geochemical significance. *Limnol. Oceanogr.* 33:702–724.
- Smith, S.V. 1984. Phosphorus versus nitrogen limitation in the marine environment. *Limnol. Oceanogr.* 29:1149–1160.
- — —, and M.J. Atkinson 1983. Mass balance of carbon and phosphorus in Shark Bay, Western Australia. *Limnol. Oceanogr.* 28:625–639.
- — —, and M.J. Atkinson 1984. Phosphorus limitation of net production in a confined aquatic ecosystem. *Nature.* 307: 626–627.
- Stocker, R., and J. Imberger. 2003. Horizontal transport and dispersion in the surface layer of a medium-sized lake. *Limnol. Oceanogr.* 48:971–982.
- Strickland, J. D. H., and T. R. Parson. 1972. *A practical handbook of seawater analysis*. Fishery Research Board, Canada.
- Switala, K. 1993. Determination of ammonia by flow injection analysis colorimetry (dialysis). Lachat Instruments, Milwaukee, USA.
- Thingstad, T. F., and others. 2005. Nature of P limitation in the ultraoligotrophic Eastern Mediterranean. *Science* 309: 1068–1071.
- Thompson, P., and A. Waite. 2003. Phytoplankton responses to wastewater discharges at two sites in Western Australia. *Marine and Freshwater Research.* 54:721–735.
- Tobias, C.R., M. Cieri, B. J. Peterson, L. A. Deegan, J. Vallino, and J. Hughes. 2003. Processing watershed-derived nitrogen in a well-flushed New England estuary. *Limnol. Oceanogr.* 48:1766–1778.
- Utermöhl, H. 1958. Zur vervollkommnung der quantitativen phytoplankton-methodik. *Mitt. Int. Ver. Limnol.* 9. 38 pp.
- Valderrama, J. 1981. The simultaneous analysis of total nitrogen and total phosphorus in natural waters. *Marine Chemistry.* 10:109–122.
- Wanninkhof, R., and others. 1997. Gas exchange, dispersion, and biological productivity on the west Florida shelf: Results from a Lagrangian tracer study. *Geophysical Research Letters* 24:1767–1770.
- Wetzel, R. 2001. *Limnology and lake and river systems*. 3rd ed. Academic Press London.
- Zaker, N. 1998. Dynamics of the coastal boundary layer off Perth, Western Australia. PhD thesis, Univ. of Western Australia.

Submitted 2 May 2006

Revised 6 August 2007

Accepted 10 September 2007